

Small, Nonstoichiometric Zinc Sulfide Clusters

Krum Chuchev and Joseph J. BelBruno*

Department of Chemistry, Dartmouth College, Hanover, New Hampshire 03755

Received: July 15, 2004; In Final Form: December 13, 2004

Recent experiments indicated that the formation of small, nonstoichiometric clusters Zn_nS_m and $Zn_nS_m^+$ was possible. In this work, the ground states of these clusters, where $1 \leq n, m \leq 4$, were studied using density functional theory. Global minima were found to be primarily cyclic structures in which the S–Zn–S preference for large bond angles was preserved. Ionization was shown to lead to structural relaxation and occasionally major changes in conformation. Cohesive energies are reported as a function of cluster composition. Qualitative comparisons were extracted from the energetics resulting from structural optimizations, and such comparisons appear to be consistent with the experiment. The computational data for the ZnS_n and Zn_nS_m (where $m > n$) clusters indicated that sulfur–sulfur bonding in larger ZnS clusters could be feasible without significant energetic cost and that such structures should at least be considered.

Introduction

The II–VI semiconductors are of interest because of their wide-ranging applications. For example, these compound semiconductors are used as catalysts,¹ as solar cells,² and in quantum devices, such as quantum dots.³ The versatility of the material has led to intense experimental efforts to quantify its physical properties and to improve performance in practical devices. Nanoparticle-sized clusters of these materials are recent experimental targets, since they exhibit size-dependent chemical and physical properties. In particular, the transition from molecular to nanoparticle and, finally, bulk properties presented by these semiconductors represents a fundamental research problem, but one that has significant practical applications. Zinc sulfide and cadmium sulfide have been the primary focus of most of the reported research. Here, we focus on small, nonstoichiometric clusters of ZnS.

A small number of computational studies have been reported for ZnS molecular clusters as well as crystallites of up to several hundred atoms. The structure of small crystallites has been explored using Hartree–Fock tight binding methods.⁴ These clusters were based on the zinc blende bulk structure of ZnS. An attempt was made to apply restricted Hartree–Fock methods to small ZnS clusters (up to eight total atoms). However, the only reported converged structure was the stoichiometric tetramer.⁵ Density functional theory (DFT) with a core pseudopotential was used in a study of small stoichiometric gas-phase clusters, $(ZnS)_n$, $n \leq 9$.⁶ For stoichiometric clusters with five or fewer monomer units, the calculations found that planar, monocyclic rings were the preferred geometry. Three-dimensional structures became important beyond this cluster size. The same authors used time-dependent DFT to optimize the low-lying excited states of the stoichiometric clusters and estimate the electronic excitation energies.^{7,8} More recently, a DFT study of the structure of mixed clusters of up to four atoms was reported.⁹ Larger stoichiometric clusters ($n > 9$) have been treated by density functional theory¹⁰ or simulated annealing,^{11,12} leading to global minima with open structures or bubble cluster geometries based on four- and six-membered rings of ZnS.

Recent mass spectrometric analysis¹⁰ of the plume created by laser ablation of mixtures of zinc and sulfur, as well as ZnS,

has indicated that, for small cluster sizes, significant quantities of nonstoichiometric clusters were produced. However, as the cluster size increased, the clusters tended to be predominately stoichiometric. The same studies have shown that anomalously large peaks occurred for stoichiometric clusters of 13 and 34 monomer units. Subsequent computational analysis of possible geometries for these stable clusters did not yield structures that could account for the seemingly increased stability found in the mass spectra.

From a different perspective, inorganic chemists have been exploring metal–sulfide bonds for quite some time. These include studies of disulfide and polysulfide bonds. However, in almost all cases, ancillary ligands are available to the coordinating metal. The many examples of reported metal–sulfur bonds include a recent characterization¹³ of RuS_2 nanoislands on Au(111), in which a distorted NaCl crystal structure was reported. In this structure, Ru was bound to discrete S_2 units, which occupied the Cl positions. Complex diruthenium complexes with a Ru_2S_2 core were also reported.¹⁴ In these structures, a rhomboid-like core with a Ru–Ru bond was observed. An analogous core forms the basis of $CpMoMn(CO)_5(\mu-S_2)$ and the related manganese complex.^{15,16} More relevant to the current work, similar results are available for zinc. For example, Verma and co-workers,¹⁷ in a novel synthetic method, report tetrahedral structures for zinc surrounded by four sulfur atoms. Zinc polysulfide complexes exhibited a range of core structures dependent on the ratio of zinc to sulfur.¹⁸ Luther et al.¹⁹ reported sphalerite-like structures for $[Zn_4S_6(H_2O)_4]^{4-}$ and $[Zn_3S_5(H_2O)_4]$. Six-membered rings were the primary feature of these geometries. Zinc polysulfide complexes $[Zn(S_4)_2]^{2-}$ were shown, by their crystal structures, to be composed of a pair of tetrahedrally coordinated bidentate ligands, with S–S bond lengths approximately equal to those of the free ligand.²⁰ Finally, a mass spectrometric fragmentation study of capped ZnS has been reported. Under normal conditions, the zinc–sulfur core was found to be stable with respect to dissociation.²¹ Six-membered rings were again the preferred structural building block. These studies, for the most part, are focused on more complex systems. In the current work, we are exploring the structures for a range of clusters that might form the cores of

analogous transition-metal complexes. However, the sulfur ligand in the current work is not limited to S_2 , S_4 , or S_6 units, but allowed to vary continuously, since the most recent mass spectrometric results were obtained using laser ablation, a process that creates an environment in which atomic constituents are readily produced.

All previous computational studies have focused on heteronuclear bonding. The experimental presence of small nonstoichiometric clusters in the recent mass spectrometric experiments was indicative of at least the *possibility* of homonuclear bonding within the larger, $n = 13$ or 34 sized clusters. The current study was carried out to explore the structure of these small clusters, both in a fundamental sense and as a possible guide to nontraditional geometries for the larger clusters.

Computational Methods

The calculations reported in this work were all completed with the Gaussian 98 suite of programs.²² In particular, the primary computational tools involved the hybrid B3LYP functional²³ with the CEP-121G basis set,^{24–26} and all reported structural results were obtained via that theoretical method. This basis set employed a relativistic effective core potential for all but the outermost electrons. A similar theoretical method has been previously employed and shown to be sufficiently accurate to explore the structures of stoichiometric zinc sulfide clusters of up to nine monomeric units.^{11,12} That research used a modified basis set that included an additional set of diffuse functions. Calculations for the neutral dimer, trimer, and tetramer clusters have been completed and reported here as a test of the accuracy of the current theoretical method. As shown in the subsequent sections, our unmodified basis set provided results nearly identical to those previously reported, indicating that the more cpu-intensive basis set that included diffuse functions was unnecessary in this work. All global minimum structures were confirmed as stationary points by calculating the harmonic frequencies at the same level of theory. For the reported structures, all of the harmonic frequencies were real and the optimized structures had the lowest total energy of all of the geometries examined for that particular stoichiometry. Electron density maps were plotted using GAUSSVIEW software.

Results

The optimized structures, using the related B3LYP/SKBJ(d) theoretical method, for stoichiometric clusters of up to eight monomer units have been previously reported.¹ We have optimized the structures of the three smallest stoichiometries and compared the resulting structures with the those of the previous study as a reference for the accuracy of the theoretical method used here. For the monomer, the calculated bond length, 2.113 Å, was shorter than the bulk value⁵ of 2.35 Å. This difference is an extreme example of the change in physical properties as the molecular ZnS evolves into the bulk form. Previous calculated bond lengths^{6,9} have been in the range from 2.05 to 2.13 Å. Our optimized structures for Zn_2S_2 , Zn_3S_3 , and Zn_4S_4 are shown in Figure 1 with the respective bond lengths and bond angles. The zinc–sulfur bond distance in the dimer was increased by nearly 10% compared to that of the monomer; however, the zinc–sulfur bond length decreased as the stoichiometric clusters grew further in size. The trend toward the bulk ZnS bond distance does not begin until cage structures are formed.

The rhomboid geometry **I** was the global minimum for the dimer. In this structure, there was an explicit zinc–zinc bond (2.474 Å) across the diagonal. This is evident in the electron

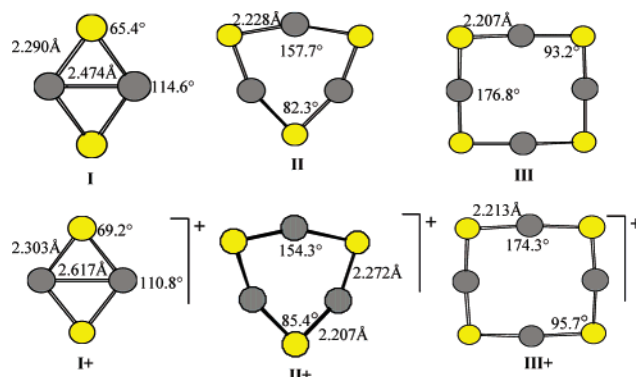


Figure 1. Global minimum structures for neutral and cationic stoichiometric clusters of up to six atoms. The darker balls represent the zinc atoms. Bond lengths and bond angles are indicated.

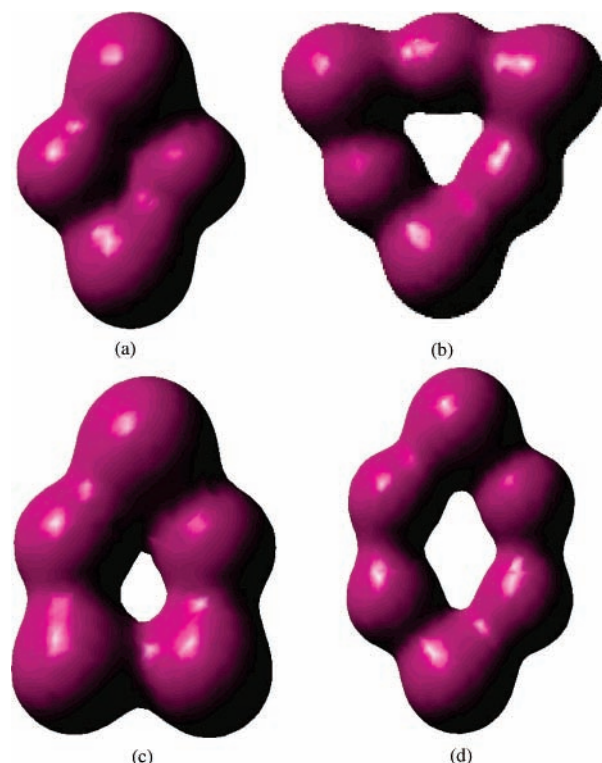


Figure 2. Total electron density maps for (a) Zn_2S_2 (**III**); (b) Zn_3S_3 (**III**); (c) Zn_2S_3 (**XXII**), and (d) Zn_4S_2 (**XXIV**).

density plot shown in Figure 2a. For the trimer, the global minimum was the six-membered ring **II** shown in the figure. The zinc–zinc distance in this structure was 2.961 Å, longer than typically observed for the metal–metal bond. The electron density plot, Figure 2b, confirms the absence of any Zn–Zn interaction. Finally, the tetramer global minimum was the nearly square, eight-membered ring **III**. The geometries for all three structures were within 1% of those previously reported. The cation geometries **I+**, **II+**, and **III+** were qualitatively identical to the structures of the neutrals. The main effect of ionization in these clusters was development of a slight asymmetry in **II+** and small modifications in the bond angles. Bond angle changes (1–4%) decreased across the series as the cluster size increased.

Approximately 200 total possible structures for the nonstoichiometric clusters Zn_nS_m , where $n, m \leq 4$, were examined. The range of starting geometries were based on the reported structures for other semiconductor clusters such as Ga_nAs_m and chemical intuition in order to include other possibilities. A selection, but not a complete inventory, of general initial

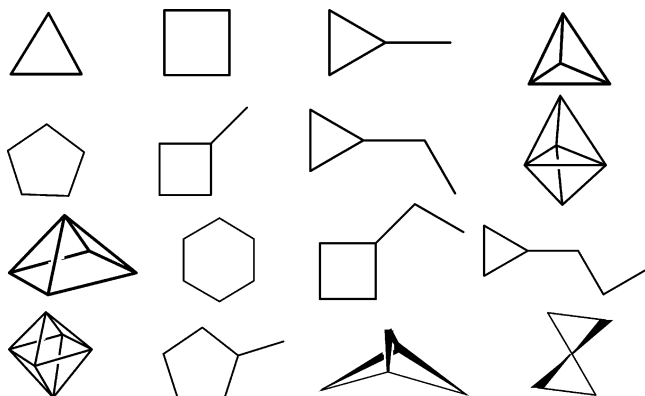


Figure 3. General structures used as initial geometries in the global minimum search. All positional permutations of the atoms were used as initial geometries for optimization. Linear and bent chains were employed, but are not shown.

geometries is shown in Figure 3. All of the possible arrangements of the atoms in these geometries were used as starting points for optimization. Not shown in the figure are numerous linear, bent, and branched chain configurations, for which all atomic permutations were optimized. Although some low-lying, three-dimensional structures were located, the global minima for all of the nonstoichiometric clusters examined in this work were planar. The lowest energy structures for all of the clusters are presented in Figures 4 and 5 with the corresponding bond lengths and bond angles. Cohesive energies are contained in Table 1. For simplicity, the clusters, both neutral and cationic, are discussed in groups determined by the total number of atoms in the cluster.

Zn₂S and ZnS₂. Because of the small cluster size, the number of possible structures was limited. However, all possibilities, cyclic, linear, and bent, were examined. The lowest energy structures are shown in Figure 4. The bond energetics led to different global minimum geometries for neutral Zn₂S and ZnS₂. For the former, the symmetric linear form **IV**, with two zinc–sulfur bonds, was 0.19 eV lower than the asymmetric linear

TABLE 1: Cohesive Energies for the Global Minimum Structures^a

cluster	<i>E</i> , kJ mol ⁻¹	cluster	<i>E</i> , kJ mol ⁻¹
ZnS	91.4	Zn ₃ S ₃ (II)	1075.8 (358.6)
Zn ₂ S ₂ (I)	542.8 (271.4)	Zn ₃ S ₄ (III)	1505.9 (376.5)
Zn ₂ S (IV)	178.5	ZnS ₂ (VII)	241.5
Zn ₃ S (IX)	213.3	ZnS ₃ (XII)	538.6
Zn ₄ S (XIV)	289.9	ZnS ₄ (XVII)	729.6
Zn ₃ S ₂ (XIX)	653.7	Zn ₂ S ₃ (XXII)	784.0
Zn ₄ S ₂ (XXIV)	715.9	Zn ₂ S ₄ (XXVII)	1003.9

^a Energies per ZnS monomer unit are in parentheses.

cluster. The zinc–sulfur bond lengths were longer than in the monomer and comparable to those in Zn₂S₂. A bent geometry was 0.43 eV higher in energy. The global minimum reflected the preference for maximizing the number of heteronuclear bonds and the relatively weak contribution of the metal–metal bonding. For ZnS₂, however, the triangular *C*_{2v} geometry **VII** was 0.25 eV lower than the symmetric linear form. With this ratio of sulfur to zinc, the triangular structure maximized the number of Zn–S bonds, while allowing for significant sulfur–sulfur interaction within the cluster. Attempts to optimize the asymmetric linear geometry led to dissociation into Zn + S₂. The cations Zn₂S⁺ and ZnS₂⁺ demonstrated structural tendencies similar to those of the neutral clusters. The asymmetric linear form **V**⁺ was the global minimum for the Zn₂S⁺ cluster ion, 0.37 eV below the symmetric cluster **VI**⁺. A cyclic form of this cluster ring-opened upon optimization. The Zn–S bond length in **V**⁺ was slightly shorter than in the neutral cluster, reflecting a more ionic bond involving a charged zinc atom. For ZnS₂⁺, the triangular *C*_{2v} geometry **VIII**⁺ was the global minimum as was observed for the corresponding neutral cluster. In the ion, the zinc–sulfur bond length increased, while the sulfur–sulfur interaction became stronger, as evidenced by a decrease in that bond length.

Zn₃S and ZnS₃. The lowest energy structures for these neutral and cationic clusters are presented in Figure 4. The geometry of the Zn₃S cluster followed from that of the Zn₂S cluster, built by the addition of a zinc atom, so that a linear conformer, **IX**,

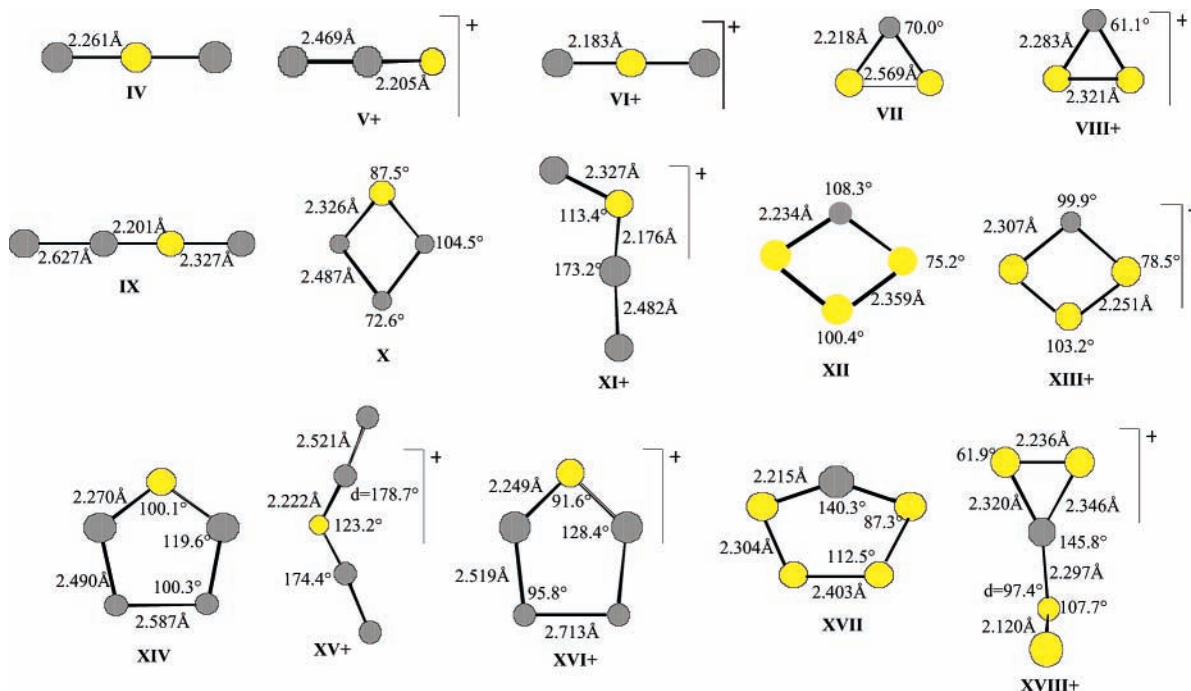


Figure 4. Global minimum structures for the ZnS_{*n*} and Zn_{*n*}S clusters. The darker balls represent the zinc atoms. Bond lengths and bond angles are indicated.

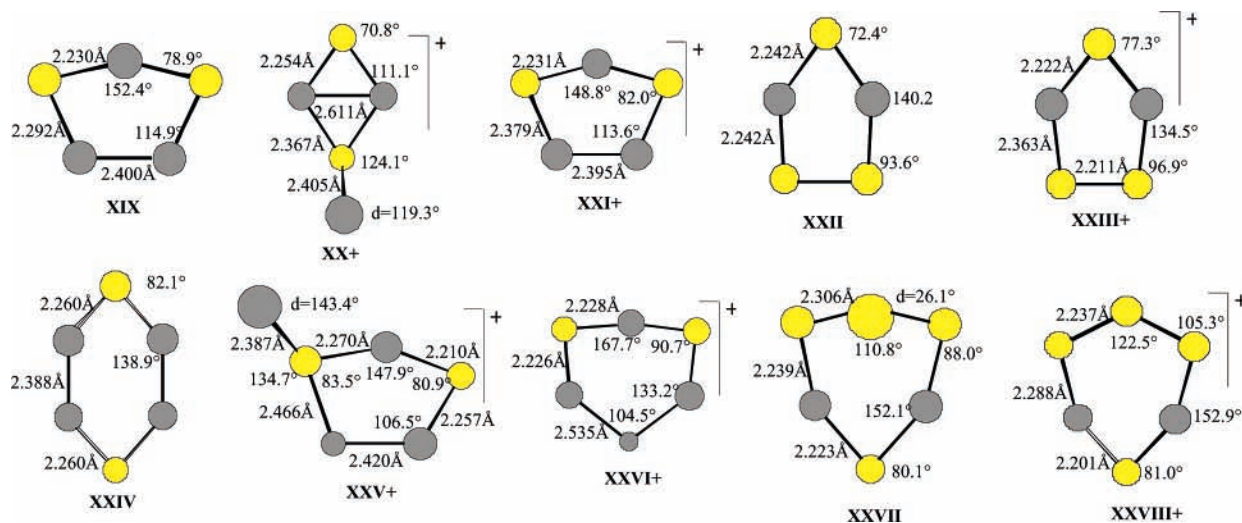


Figure 5. Global minimum structures for the Zn_2S_n and Zn_nS_2 clusters. The darker balls represent the zinc atoms. Bond lengths and bond angles are indicated.

with unequal zinc–sulfur bond lengths, was the global minimum. Other low-lying structures included a rhomboid geometry, **X**, analogous to the ZnS_3 structure, that was only 0.08 eV above the linear form and three-membered ring and branched forms that were 0.24 and 0.33 eV higher in energy, respectively. As was true for the three-atom clusters, the geometric preference was a reflection of the ineffectiveness of the zinc–zinc interaction. The ZnS_3 global minimum was the rhomboid structure **XII**, which represented the addition of a sulfur atom to the global minimum C_{2v} ZnS_2 structure. The other conformers were significantly higher in energy. For example, a bent chain structure was 0.88 eV, and the linear chain 1.86 eV, above this global minimum energy. The zinc–sulfur bond length was less than that of the stoichiometric dimer, and comparable to that observed for the three-atom clusters. In the case of the cations, Zn_3S^+ qualitatively followed the structural tendencies of its neutral precursor; however, a bent, **XI**⁺, rather than linear, chain was the lowest energy conformer with branched, linear, and rhomboid forms 0.11, 0.34, and 0.53 eV above the global minimum. Zn_3S^+ exhibited the same structural preference as the neutral cluster. The rhomboid ion **XIII**⁺ was the lowest energy structure, and the bent and linear chains were significantly higher, 0.54 and 1.01 eV, in energy. The zinc–sulfur bond is lengthened and the sulfur–sulfur bond shortened in the ion. This weakening of the heteronuclear bond and strengthening of the homonuclear interaction were also observed for the three-atom cluster ions.

Zn_4S and ZnS_4 . The lowest energy structures for these neutral and cationic clusters are presented in Figure 4. For both clusters, the five-membered ring was the minimum energy structure. For Zn_4S , **XIV** was the first nonlinear, Zn_nS global minimum. This cyclic structure was 0.53 eV below the symmetric linear chain. The cyclic structures were now energetically competitive because the cluster size was sufficient for supporting larger and more favorable S–Zn–S bond angles. In the case of the ZnS_4 cluster, the five-membered ring **XVII**, formed by addition of a sulfur atom to the ZnS_3 cluster, was 0.70 eV more stable than a structure that resembled a pair of isosceles triangles with a common (zinc) point. For the ions, a bent form of the symmetric Zn_4S chain, **XV**⁺, was slightly more stable, by 0.14 eV, than the cationic five-membered ring **XVI**⁺. A nonplanar structure that included a three-membered ring, **XVIII**⁺, was the minimum energy Zn_4S^+ cluster. It was 0.48 eV more stable than a nonplanar four-membered ring. Ionization and the resultant

charge distribution clearly played a significant role in the geometry change from that of the neutral cluster.

Zn_3S_2 and Zn_2S_3 . The general preference for planar, five-membered ring global minima continued with this series of neutral clusters. However, some differences were present in a comparison between the geometries of the two specific clusters. The structures are shown in Figure 5, and both were readily identified as the addition products of single atoms to the rhomboid, stoichiometric dimer cluster geometry. In the case of the Zn_3S_2 cluster, the monocyclic five-membered ring **XIX** was 0.63 eV more stable than a four-membered ring alternative. For Zn_2S_3 , the cyclic geometry **XXII** was a sulfur-capped quadrilateral. The Zn–Zn distance, 2.65 Å, offers the possibility of a weak bonding interaction across the ring. However, the electron density map in Figure 2c indicates the absence of any metal–metal bonding. This structure was 1.9 eV more stable than a planar four-membered ring. The Zn_3S_2 cation had two low-energy forms; one was qualitatively the same planar ring structure that was the global minimum for the neutral cluster, **XXI**⁺, but this cation was 0.16 eV higher in energy than the nonplanar four-membered ring **XX**⁺. The Zn_2S_3 cation **XXIII**⁺ maintained the same general structure as the neutral cluster, with an increase in the internal angles so that the zinc–zinc separation is even greater than in the neutral. This structure was 1.2 eV more stable than a bipyramidal form with the sulfur atoms along the pyramid base.

Zn_4S_2 and Zn_2S_4 . Monocyclic rings were the preferred structures, and conceptually, both were products of atom insertion into a zinc–sulfur bond of the corresponding lower cluster. The Zn_4S_2 hexagonal six-membered ring **XXIV** was lower in energy, by 0.27 eV, than a shieldlike ring structure. The plot of electron density shows the absence of any Zn–Zn bonding in this cluster. This geometry reflected the extreme variability in sulfur bond angles. For Zn_2S_4 , a nonplanar, shieldlike, six-membered ring, **XXVII**, was 0.53 eV lower in energy than a symmetric cyclic structure. The S–Zn–S bond angles were approaching linear values. The $Zn_4S_2^+$ ion had two essentially isoenergetic structures. A five-membered ring, **XXV**⁺, was the global minimum, but the shieldlike six-membered ring **XXVI**⁺ was only 0.06 eV higher in energy. The $Zn_2S_4^+$ ion **XXVIII**⁺ followed the same structural pattern as the neutral cluster with similar energy differences between the

two isomeric forms. There was a shortening of the bonds involving the apex atoms and a lengthening of the remaining bonds.

Discussion

The stoichiometric cluster energies followed the pattern reported in an earlier computational study. The cohesive energy (per monomer unit) in Table 1 was observed to increase with cluster size. The extrapolated value, from this small number of clusters, for the cohesive energy of bulk ZnS, $n = \infty$, was approximately 560 kJ mol^{-1} . This compared favorably with the experimental value of 607 kJ mol^{-1} .¹

Comparisons of the cohesive energies of the global minima for the nonstoichiometric clusters cannot be accomplished with the standard per monomer unit definition. Instead, we compared the absolute cohesive energies, E_{coh} . That is, the difference $E_{\text{coh}} = nE_{\text{Zn}} + mE_{\text{S}} - E(\text{Zn}_n\text{S}_m)$ was employed. Consider first the Zn_nS series of clusters. The cohesive energy of the Zn_2S cluster was approximately twice that of the ZnS monomer. This was expected, since it is a linear symmetric structure. The Zn_3S cluster was also linear. The cohesive energy for this cluster was approximately 35 kJ mol^{-1} greater than that of Zn_2S . Since the number of zinc–sulfur bonds remained constant, the additional energy was attributed to the zinc–zinc bond. The Zn_4S cluster represented the starting point of a geometry change to monocyclic rings, and analysis of the energetics must take this into account; the change to cyclic structures could have a significant impact. From a simple additive standpoint, however, there were two zinc–sulfur and three zinc–zinc bonds. We expected, on the basis of a simple bond energy argument, that the cohesive energy of this cluster would be approximately 70 kJ mol^{-1} greater than that of its predecessor **IX**, and Table 1 indicates that this is indeed the case. It appeared that either the geometry change was not a critical factor or that there were compensating effects in the cluster that provided this result. Given the propensity of S–Zn–S bonds for bond angles close to 180° and the relatively constrained ($\sim 120^\circ$) angles in the global minimum conformer **XIV**, one would conclude that there were indeed compensating energetic factors. A comparison of the cohesive energies for the stoichiometric dimer and the Zn_3S_2 cluster **XIX** confirmed this conclusion. The Zn_3S_2 cluster had four mixed bonds, as did the stoichiometric dimer. The additional metal–metal bond in the Zn_3S_2 cluster would be expected to contribute $\sim 35 \text{ kJ mol}^{-1}$. However, the total cohesive energy of **XIX** was approximately 110 kJ mol^{-1} greater than this predicted value. One S–Zn–S bond angle in **XIX** was 152° in comparison to the 114° bond angle in the stoichiometric cluster **II**. The added stability, beyond simple additive bond energies, may be attributed to this more favorable geometry. Moving to the final, Zn_4S_2 cluster, all of the S–Zn–S bond angles were increased over those in the stoichiometric dimer, and again, we found the added stability reflected in the cohesive energy.

The cohesive energies of the analogous ZnS_x clusters were uniformly higher. All of these clusters were cyclic. Begin by considering the increase in cohesive energy as sulfur atoms were added to the ZnS_2 cluster. The addition of a sulfur atom to **VII** to form ZnS_3 led to an increase in the cohesive energy of nearly 300 kJ mol^{-1} . In terms of diatomic bonding, this additional atom added only a single sulfur–sulfur bond. We, therefore, attributed most of the change in cohesive energy to formation of a S–S bond. This was consistent with the typical energy of such a bond (250 kJ mol^{-1}). Addition of yet another sulfur atom to form ZnS_4 had the same effect in terms of one additional S–S

bond and the corresponding added cohesive energy. Consideration of the simplest cluster in this series, ZnS_2 , provided an additional piece of data. The total cohesive energy of this cluster was significantly less than expected on the basis of bond energetics. There were two zinc–sulfur bonds as well as a sulfur–sulfur bond. On the basis of the previous bond energy discussion, a cohesive energy on the order of $350\text{--}400 \text{ kJ mol}^{-1}$ would be predicted. However, the S–Zn–S bond angle was 70° , and the resultant ring strain reduced the final cohesive energy considerably. The cohesive energies of the Zn_2S_3 and Zn_2S_4 clusters were consistent with the previous discussion. In the former, the strain energy was in competition with the added bond energy, while, in the latter, the improvement in geometry led to a substantial increase in cohesive energy.

Quantitative comparisons of the mass spectrometric peak intensities² with cohesive energies calculated in this work are not easily made. The peaks for the various clusters appeared in different regions of the time-of-flight spectrum, and no internal calibration was employed. However, a qualitative comparison may be undertaken by using the total peak area at a given mass and the distribution of clusters within a given mass peak as defined in the experimental work. That comparison indicated a correlation between the calculated cohesive energies and the relative amount of the molecular ions in the mass spectrum. For example, the product yield ratio of ZnS_4 to Zn_2S_2 indicated a small, but significant excess of the latter. This was reflected in their cohesive energies, which differed by $\sim 200 \text{ kJ mol}^{-1}$. Zn_2S_3 was present in much greater yield than was Zn_3S , as expected from the fact that the former had approximately 3 times the cohesive energy. These comparisons suffered from the absence of the consideration of kinetic effects. Clearly, the ablation of ZnS would produce substantial yields of the zinc sulfide monomer as well as the atomic constituents. Stoichiometric dimers should be present within the ablation plume in yields greater than indicated by their relative cohesive energies. Similarly, preliminary calculations indicated that certain reactions expected to occur in the plasma created by the laser ablation have reaction barriers, while others do not. Overall, qualitative comparisons were all that may be extracted from the thermodynamic data resulting from structural optimizations, but such comparisons appear to be consistent with the experiment.

Comparisons with the structures of the previously reported zinc sulfide and zinc polysulfide complexes are interesting. As discussed in the literature,^{20,21} the clusters are indeed stable entities. However, for the smallest clusters, the computational results provide global minima that differ from the related crystallography results. For all sulfur-rich clusters, the S–S bond length is typically near 2.30 \AA . This is significantly less than that of the S_2 molecule, but similar to the bond lengths reported in the synthetic studies. The ZnS_2 cluster geometry is indeed similar that of the RuS_2 nanoislands, that is, a metal atom interacting with an S_2 molecule. However, this is the only cluster with a geometry that may be traced back to the synthetic complexes. We find ZnS_3 to be monocyclic, but the geometry around the zinc atom is close to tetrahedral. It is unclear whether the tendency of zinc to take on such a geometry or the favorable energetics of sulfur–sulfur bonding is the driving force for this structure. The ZnS_4 cluster is also monocyclic. From the crystallographic data one might predict a tetrahedral zinc center bonded to two S_2 molecules, much like the final generic structure shown in Figure 3. However, such a structure was calculated to be $\sim 0.7 \text{ eV}$ greater in energy. Nor do we find a connection with the crystallographic results in clusters such as Zn_2S_3 . Our

calculated monocyclic structure differs from the observed¹⁹ three-dimensional structure (see the next to last generic structure in Figure 3) for $[\text{Zn}_2\text{S}_3(\text{H}_2\text{O})_2]^{2-}$. Finally, the Zn_2S_4 geometry in the current work is not related to the types of structures reported for dimanganese, -ruthenium, or -molybdenum complexes.^{14–16} These differences may be attributed to the absence of the ancillary ligands. In some of the previously studied complexes, the sulfur atoms are contained in larger organic molecules. In others, the transition metal is also bonded to large organic ligands. The calculated structures here are essentially the naked cores of these complexes. In the absence of steric factors driving a particular geometry, only energetics remain a critical factor.

One of the original motivating factors for this study was to explore the possibility of zinc–zinc and sulfur–sulfur bonding in larger clusters. Although we have not included the larger clusters, such as $n = 13$ and $n = 33$, in these calculations, we can use the results to examine the feasibility of the formation of clusters in which not all of the bonding is via Zn–S linkages. We accomplish this by comparing the cohesive energies of excess zinc and excess sulfur clusters with the cohesive energies for the stoichiometric clusters with the same number of atoms in which the bonding is all heteronuclear. On the basis of the cohesive energies in Table 1 and the corresponding structures in the figures, one may safely rule out Zn–Zn bonding as a significant energetic driving force in larger clusters. The cohesive energies for clusters with excess zinc are substantially less than those of stoichiometric clusters with an identical number of atoms. For example, compare the dimer with Zn_3S and the trimer with Zn_4S_2 . There would not appear to be any substantial energetic driving force for the experimental production of significant amounts of such nonstoichiometric clusters; formation must result from the relative concentrations of the atoms in the local environment or from kinetic effects. However, it appears from the computational data for the ZnS_n and Zn_mS_m (where $m > n$) clusters that sulfur–sulfur bonding in larger clusters could be feasible without significant energetic cost. For example, the stoichiometric dimer cluster and the ZnS_3 cluster, each with four atoms, have nearly identical cohesive energies, as do the stoichiometric trimer and the Zn_2S_4 cluster. These simple comparisons provide an energetic basis for the observed excess sulfur clusters in the mass spectrometric observations. Of course, if a large, $n \approx 13$, cluster exhibited homonuclear bonds, it would have both S–S and Zn–Zn bonds. The calculations here indicate that the former are essentially energetically neutral with respect to the energy of formation of the cluster, while the latter are energetically costly to cluster production. There is no present experimental evidence that such

clusters exist. The overall conclusion, however, is that such clusters may be feasible, if a geometry includes multiple sulfur–sulfur bonds, and that the search for the possible geometries of the larger, stable clusters should include such possibilities.

References and Notes

- (1) Hoffman, A. J.; Mills, G.; Yee, H.; Hoffmann, M. R. *J. Phys. Chem.* **1992**, *96*, 5546.
- (2) Toukova, J.; Kindl, D.; Tousek, J. *Thin Solid Films* **1997**, *293*, 533.
- (3) Cochran, E. *Sci. Am.* **1990**, *263*, 74.
- (4) Muili, J.; Pakkanen, T. A. *Surf. Sci.* **1996**, *364*, 439.
- (5) Gurin, V. S. *Solid State Commun.* **1998**, *108*, 389.
- (6) Matxain, J. M.; Irigoras, A.; Ugalde, J. M. *Phys. Rev. A* **2000**, *61*, 53201.
- (7) Matxain, J. M.; Irigoras, A.; Fowler, J. E.; Ugalde, J. M. *Phys. Rev. A* **2000**, *63*, 013202.
- (8) Matxain, J. M.; Irigoras, A.; Fowler, J. E.; Ugalde, J. M. *Phys. Rev. A* **2001**, *64*, 013201.
- (9) Katircioglu, S.; Erkoc, S. *THEOCHEM* **2001**, *546*, 99.
- (10) Burnin, A.; BelBruno, J. J. *Chem. Phys. Lett.* **2002**, *362*, 341.
- (11) Spano, E.; Hamad, S.; Catlow, C. R. *J. Phys. Chem. A* **2003**, *107*, 10337.
- (12) Spano, E.; Hamad, S.; Catlow, C. R. *Chem. Commun.* **2004**, 864.
- (13) Cai, T.; Song, Z.; Rodriguez, J. A.; Hrbek, J. *J. Am. Chem. Soc.* **2004**, *126*, 8886.
- (14) Nishibayashi, Y.; Imajima, H.; Onodera, G.; Hidai, M.; Uemura, S. *Organometallics* **2004**, *23*, 26.
- (15) Adams, R. D.; Captain, B.; Kwon, O.; Pellechia, P. J.; Sanyal, S. *J. Organomet. Chem.* **2004**, *689*, 1370.
- (16) Adams, R. D.; Miao, S.; Smith, M. D. *Organometallics* **2004**, *23*, 3327.
- (17) Verma, A. K.; Rauchfuss, T. B.; Wilson, S. R. *Inorg. Chem.* **1995**, *34*, 3072.
- (18) Pafford, R. J.; Rauchfuss, T. B. *Inorg. Chem.* **1998**, *37*, 1974.
- (19) Luther, G. W.; Theberge, S. M.; Rickard, D. T. *Geochim. Cosmochim. Acta* **1999**, *63*, 3159.
- (20) Coucouvanis, D.; Patil, P. R.; Kanatzidis, M. G.; Baenziger, N. C. *Inorg. Chem.* **1985**, *24*, 24.
- (21) Lover, T.; Henderson, W.; Bowmaker, G. A.; Seakins, J. M.; Cooney, R. P. *Inorg. Chem.* **1997**, *36*, 3711.
- (22) Gaussian 98, Revision A.11: Frisch, M. J.; Trucks, G. W.; Schlegel, H. B.; Scuseria, G. E.; Robb, M. A.; Cheeseman, J. R.; Zakrzewski, V. G.; Montgomery, Jr., J. A.; Stratmann, R. E.; Burant, J. C.; Dapprich, S.; Millam, J. M.; Daniels, A. D.; Kudin, K. N.; Strain, M. C.; Farkas, O. Tomasi, J.; Barone, V.; Cossi, M.; Cammi, R.; Mennucci, B.; Pomelli, C.; Adamo, C.; Clifford, S.; Ochterski, J.; Petersson, G. A.; Ayala, P. A.; Cui, Q.; Morokuma, K.; Malick, D. K.; Rabuck, A. D.; Raghavachari, K.; Foresman, J. B.; Cioslowski, J.; Ortiz, J. V.; Stefanov, B. B.; Liu, G.; Liashenko, A.; Piskorz, P.; Komaromi, I.; Gomperts, R.; Martin, R. L.; Fox, D. J.; Keith, T.; Al-Laham, M. A.; Peng, C. Y.; Nanayakkara, A.; Gonzalez, C.; Challacombe, M.; Gill, P. M. W.; Johnson, B.; Chen, W.; Wong, M. W.; Andres, J. L.; Gonzalez, C.; Head-Gordon, M.; Replogle, E. S.; Pople, J. A., Gaussian, Inc., Pittsburgh, PA, 1998.
- (23) Becke, A. D. *J. Chem. Phys.* **1993**, *98*, 5648.
- (24) Stevens, W. J.; Basch, H.; Krauss, H. M. *J. Chem. Phys.* **1984**, *81*, 6026.
- (25) Stevens, W. J.; Krauss, M.; Basch, H.; Jasien, P. G. *Can. J. Chem.* **1992**, *70*, 612.
- (26) Cundari, T. R.; Stevens, W. J. *J. Chem. Phys.* **1993**, *98*, 5555.